

## Synergistic Enhancement of Hydrophilicity in Silk Fibroin/Linen Blends via Polyethylene Glycol and Curcumin for Advanced Wound Healing

Fatemeh Rafati, Narges Johari\*

\* *n.johari@iut.ac.ir*

<sup>1</sup> Materials Engineering group, Golpayegan College of Engineering, Isfahan University of Technology, Golpayegan, Iran

Received: June 2025

Revised: September 2025

Accepted: September 2025

DOI: 10.22068/ijmse.4116

**Abstract:** It must be recognised that the degree of this factor will influence how well wound-healing materials perform in water absorption, protein interaction, and cellular adhesion. In the present study, we are concerned with studying the effects of polyethylene glycol (PEG) and curcumin (Cur) on the hydrophilicity of silk fibroin (SF)/linen (LN) composite films. The SF and LN composite films were blended at an equal mass ratio of 1:1, and PEG and Cur were also added to induce changes in surface properties. Fourier-transform infrared analyses showed that intermolecular interactions and hydrogen bonding were formed among the components in the blends. There was a pronounced hydrophobicity reduction by the addition of Cur and PEG/Cur, as exemplified by the static water contact angle measurements: simply the addition of Cur to SF lowered the contact angle from approximately 100° to 72°, whereas a co-addition of PEG and Cur produced the most significant reduction (64°), equalling 70%. The synergistic effect in the surface wettability enhancement occurs because both additives introduce polar moieties onto the surface and partially disrupt the SF crystalline structure. Water uptake and cell viability tests further verified the hydrophilicity and biocompatibility of PEG/Cur-modified SF/LN films. This promotes the use of PEG/Cur-modified SF/LN blends as hydrophilic, bioactive materials suited for advanced wound dressing and tissue engineering scaffolds.

**Keywords:** Silk fibroin, Linen, Polyethylene glycol, Curcumin, Hydrophilicity, Surface wettability.

### 1. INTRODUCTION

Wound healing is quite a highly intricate and dynamic biological process that involves several cellular and molecular events, including homeostasis, inflammation, proliferation, and remodelling [1, 2]. It is, therefore, essential to design effective wound dressings and tissue scaffolds to aid and enhance this process [3]. Within various materials considered for biomedical applications, silk fibroin (SF) has become a very promising biopolymer, mainly due to its excellent biocompatibility, biodegradability, minimal inflammatory response, and tunable mechanical properties. Silk fibroin originates from the cocoons of *Bombyx mori* silkworms, hence providing silk fibroin with an unusual protein structure that promotes cell adhesion and growth, while modifying its film-forming ability and structural integrity tailored towards tissue engineering [4-6].

Despite these advantages, one of the limitations of pure SF is its relatively hydrophobic surface, which can restrict both water absorption and cellular infiltration within moist environments of wounds. Such a fact has called for the recent efforts in research to modify SF with another

hydrophilic natural or synthetic polymer to optimize its biological performance and moisture-handling characteristics. Combining SF with other functional biopolymers thus opens yet another promising approach towards tailoring its physico-chemical and biological properties according to specific clinical needs [7-10]. More accurately, linen (LN), being an extract from flax fibers, is considered renewable and plant-derived and has impressive biological activities at the same time. In fact, several bioactive compounds are embedded in this matrix, like lignans, phenolics, and polysaccharides, and they provide anti-inflammatory, anti-platelet, and antioxidant properties [11-13]. These properties are essential in wound therapies to reduce inflammation, facilitate angiogenesis, and accelerate tissue regeneration. Besides, owing to the high concentration of hydroxyl groups that can establish immense hydrogen bonding with water molecules and other polymers, LN is hydrophilic in nature [14, 15].

LN imparts hydrophilicity, and construction like that of a support using an SF matrix may bring other parallel biological benefits. For instance, hydrogel scaffolds combining cellulose and linseed gum (a flaxseed derivative) have been

shown to exhibit reduced water contact angles due to continuous hydrogen-bond formation between cellulose chains and linseed gum molecules, as reported by Deng et al. [16]. Therefore, it is concluded that such flax-based materials could be further promising in hydrophilic and bioactive scaffold design.

Contact angle aspirations are frequently used to assess hydrophilicity, which is an essential factor in interfacial behaviour between biomaterials and the biological environment. Generally, the wetting property of a lower angle indicates stronger protein adsorption, cell spreading, and absorption of exudate from wounds. Hence, optimization of hydrophilic properties of SF-based composites is a necessary step to enhance the performance occurring in wound healing and tissue engineering applications [17-19].

To improve hydrophilicity, polyethylene glycol (PEG) and curcumin (Cur) are exciting. PEG is a well-known hydrophilic polymer that increases water absorption and affords surface wettability to the composite systems. Curcumin could also be bonded to the polymer chains via a hydrogen link with  $\pi$ - $\pi$  interaction, thereby modifying the surface characteristics and bioactive nature of the material [20-26].

This study will focus on how PEG and curcumin affect the hydrophilic behaviour of SF/LN blends. The prepared films were analysed using Fourier-transform infrared spectroscopy to confirm structural interactions and contact angle measurements to check surface wettability. Imparting target hydrophilicity to SF/LN-based materials through suitable blending will further enhance this research, leading to the development of more effective biomaterials for wound healing applications.

## 2. EXPERIMENTAL PROCEDURES

### 2.1. Materials

The degummed SF was obtained from *Bombyx mori* cocoons according to the standard degumming procedure. LN powder was prepared from flax fibers by powdering them to a fine, uniform powder in a grinder and sieve. PEG (Mw $\approx$  400 g/mol) and Cur >99% purity were purchased from Sigma-Aldrich, USA and used without any further purification. Lithium bromide (LiBr, Merck, Germany) and dialysis membranes (with a molecular weight cut off of 14 kDa) were purchased from Sigma-Aldrich, USA.

### 2.2. Preparation of Silk Fibroin Solution

To prepare fibroin from silk, the silk fibres must first be degummed to remove sericin. Three open silkworm cocoons were boiled for one hour in a 0.02 M sodium carbonate solution. The degumming silk fibers were then washed several times with cold and hot deionized water and rinsed thoroughly. They were then dried for 24 hours at ambient conditions. To prepare fibroin, the degummed silk fibres were added to a 9.3 M LiBr solution at a ratio of 10% w/v and dissolved at 60°C for 4 hours. The concentrated salt and fibroin solution was placed in a dialysis tubing (Sigma-Aldrich, USA) with an outlet coefficient of 14 kDa for 72 hours in deionized water. The deionized water in the dialysis tubing container was changed regularly at 4-hour intervals [27]. The remaining solution in the dialysis tubing was centrifuged, yielding a pure SF solution with a concentration of 2 %w/v.

### 2.3. Preparation of SF/LN Blends

Equal volumes of SF and LN solutions were mixed under magnetic stirring for two hours at room temperature to yield an SF/LN homogeneous blend. The LN powder that was previously pre-dispersed and ultrasonicated for 15 minutes in deionized water ensured uniform dispersion before the mixing of the SF solution [11].

### 2.4. Incorporation of PEG and Curcumin

To find out the effect of PEG and Cur on the hydrophilicity of blends, 5 ml of PEG and 0.0001 g of Cur were added to the SF/LN blend while stirring gently [28, 29]. The mixture was stirred continuously for 2 hours to allow optimal mixing and interaction between the components. Cur was pre-dissolved in a minimal volume of ethanol to increase dispersion in the aqueous blend, and then added dropwise into the mixture. The final blends were cast into Petri dishes and dried at 40°C in a vacuum for 24 hours to obtain thin films. The dried films were peeled off and stored in desiccators until further characterization [30, 31].

### 2.5. Characterization

The samples have been characteristically and chemically analysed with Fourier Transform Infrared Spectroscopy (FTIR, MB series, ABB Bornem, Canada) within the spectral range of 400-4000  $\text{cm}^{-1}$ . For surface wettability measurements, the samples were applied with a water drop of 5  $\mu\text{L}$  while

using a goniometer (KRÜSS DSA100) to measure the contact angle formed. All values reported for an experiment were the average of three readings made at different parts of a sample. All such tests were done at room temperature ( $22 \pm 2^\circ\text{C}$ , relative humidity of 40–50%).

The morphologies of the prepared porous functionally graded SF/LN composite were studied by Field Emission Scanning Electron Microscopy (FESEM; MIRA3SACN-XMU, Czech Republic). The gold-coated SF/LN composite was examined in FESEM at 30 kV and 2  $\mu\text{A}$ .

The fusion of the MTT stock was prepared to 5 mg/mL by dissolving 50 mg in 10 mL of PBS in a sterile reagent tube and kept in the dark at  $4^\circ\text{C}$ . MTT was incubated before use for 1 hour at  $37^\circ\text{C}$  and passed through a sterile syringe filter of 0.2  $\mu\text{m}$  pore size to eliminate any crystals formed. For the assay, 200  $\mu\text{L}$  whole culture medium containing  $1 \times 10^4$  Human dermal fibroblasts was seeded into each well of a 96-well plate. After incubation at  $37^\circ\text{C}$  for 12–24 hours, the cells were 40–60% confluent. To continue, cells were incubated at  $37^\circ\text{C}$  for 24 hours in the presence of 200  $\mu\text{L}$ /well of test extract (and controls). After disposing of the medium containing the test extract, the wells were washed twice with warm PBS at  $37^\circ\text{C}$ . Subsequently, fresh medium (180  $\mu\text{L}$ ) and MTT solution (20  $\mu\text{L}$ ) were added to every well, to a final MTT concentration of 0.5 mg/mL. After 4 hours of incubation at  $37^\circ\text{C}$ , the medium was carefully aspirated, and 100  $\mu\text{L}$  dimethyl sulfoxide (DMSO; Sigma-Aldrich, USA) was added to each well to dissolve the purple formazan crystallization. The plates were gently shaken to allow for complete solubilization. The optical density (OD) was measured using a multiwell plate reader (Anthos 2020, Germany) at a reference wavelength of 690 nm and a test wavelength of 540 nm. Data are presented as percentages from untreated controls, with different concentrations of test chemicals. Samples of the three groups were analysed in triple tests [32, 33]. Cell viability was calculated based on Equation 1, where "OD of sample" refers to absorbance for the nanocomposite hydrogel solution, while "OD of control" is for the control sample [32].

$$\% \text{ Cell viability} = \frac{\text{OD of sample}}{\text{OD of control}} \times 100 \quad (1)$$

### 3. RESULTS AND DISCUSSION

Figure 1 represents the FTIR spectra of the

synthesized SF/LN variegated blends containing and excluding PEG and Cur. It is clear from the spectra that the different functional groups correspond to the polymer and additive constituents. The amide I, II, and III bands corresponding to silk fibroin are at around 1650  $\text{cm}^{-1}$ , 1540  $\text{cm}^{-1}$ , and 1240  $\text{cm}^{-1}$ , respectively, suggesting that  $\beta$ -sheet structures are present [34, 35]. LN, which is composed mainly of cellulose-like compounds, has two characteristic absorption bands in the spectral area of 1025–1050  $\text{cm}^{-1}$ , which are due to C–O stretching, and also shows a broad O–H stretching band at about 3300  $\text{cm}^{-1}$  due to hydroxyl groups [36, 37]. The blending of SF and LN yields observable shifts and broadening of these peaks, suggesting hydrogen bonding between the two components. Also noted by Zhang et al. [38], such blending leads to extremely diversified hydrogen bonds with different bond strengths and lengths, which is reflected in the spectral changes. The introduction of PEG has resulted in an apparent increase in the intensity of the O–H stretching band, which is further confirmed by evidence for the presence of abundant hydroxyl groups coming from common PEG chains [39, 40]. It also goes with a slight peak sharpness decrease around 1640  $\text{cm}^{-1}$ , suggesting a disruption in SF crystallinity due to hydrogen bonds between PEG and protein chains [39, 41]. Samples containing Cur have displayed significant variation in the 1200–1300  $\text{cm}^{-1}$  region. The intense peak at 1281  $\text{cm}^{-1}$  in control blends was found to broaden and split into more subtle peaks, which can be attributed to hydrogen bonding involving the enolic OH groups of curcumin. While  $\pi$ – $\pi$  interactions have been proposed in similar systems, FTIR data alone cannot confirm this mechanism. Complementary techniques such as UV–Vis or fluorescence spectroscopy would be required for direct evidence, which will be pursued in future studies [42]. These spectral features showed successful incorporation of Cur within the blend as well as interaction with both SF and LN components.

In the FESEM images, Figure 2 depicts SF, LN, and the composite blends containing PEG and Cur. These micrographs serve to provide clues into the microstructural evolution of the materials and the changes in surface wettability, which are very important for biomedical performance and moisture-regulating wound dressings [43]. Figure 2a presents a highly compact and smooth surface

morphology consistent with a dense protein matrix interspersed by  $\beta$ -sheet crystalline structures. Such microstructural organization permits the assembly of a factorially dense, low-porosity surface with less exposure to hydrophilic functional groups.

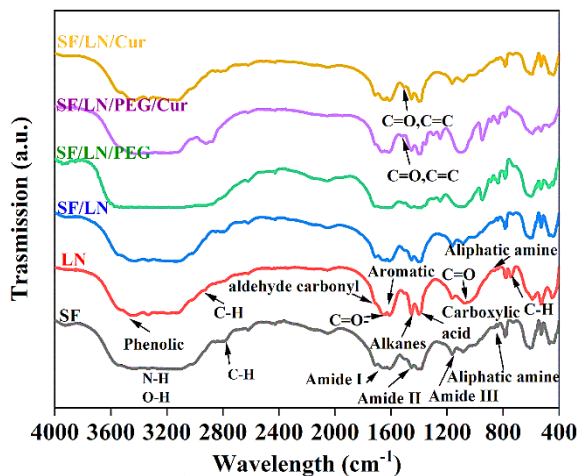
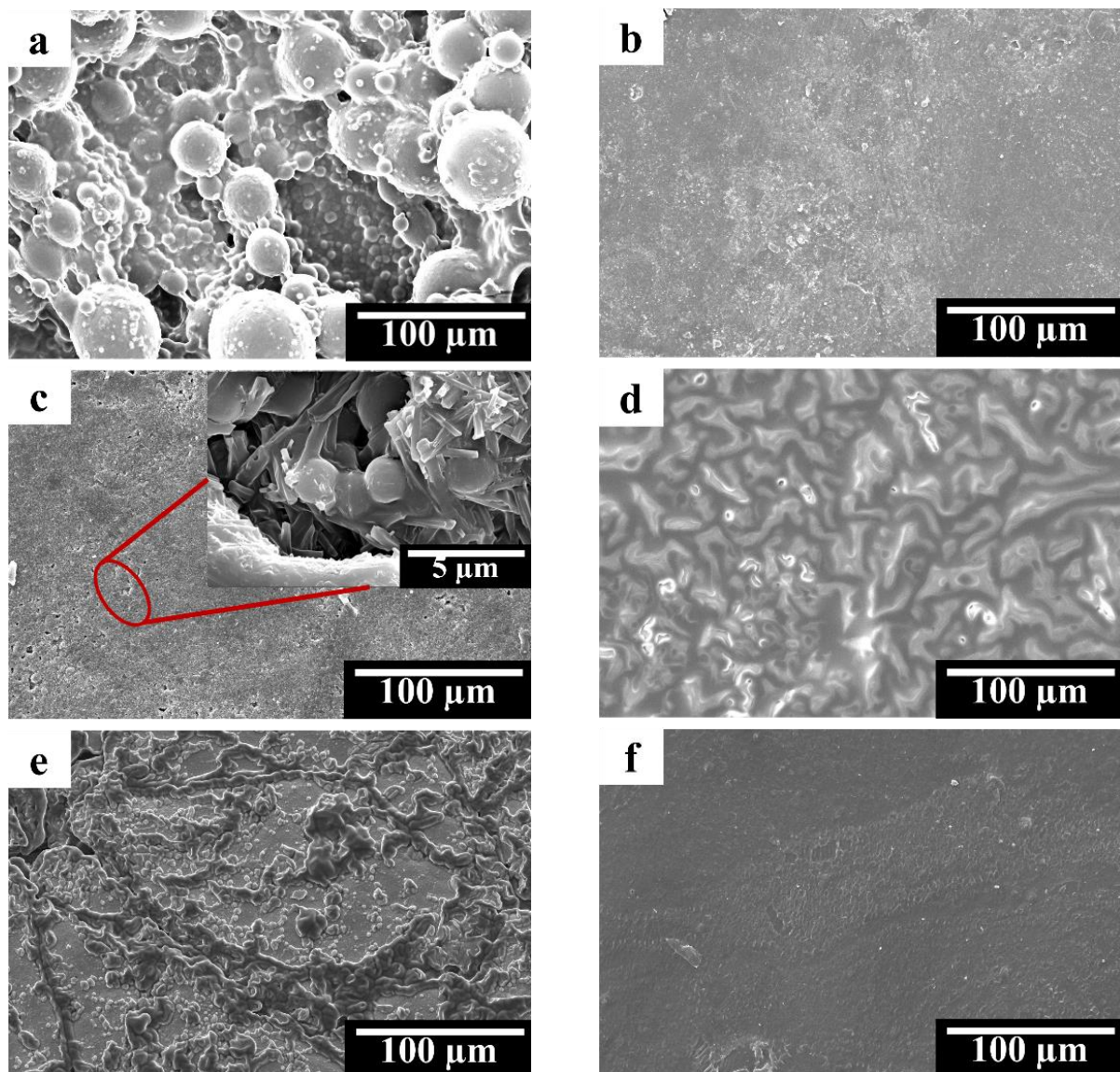


Fig. 1. FTIR spectra of SF/LN blends

Therefore, the pure SF has an average static water contact angle of  $\sim 100^\circ$ , asserting its hydrophobic nature. These findings are consistent with heterogeneous wetting behavior, where surface roughness and lack of polar functionality contribute to increased hydrophobicity [44, 45]. Figure 2b exposes a fibrous, irregular topography. LN, mainly cellulose and related polysaccharides, has a vast density of -OH groups capable of forming extensive network bonding interactions with water. The presence of surface roughness and chemical polarity results in a substantial reduction in the water contact angle compared to SF, thus making LN an inherently hydrophilic material. Being hydrophilic, this facilitates the enhancement of wettability for SF-based systems [46, 47]. The SF/LN composite (Figure 2c) shows a somewhat semi-homogeneous mixed morphology, wherein fibrous LN structures are partially embedded in the SF matrix. Blending establishes hydrogen bonding interactions between SF amide groups and LN hydroxyl groups. This disrupts the  $\beta$ -sheet packing and increases surface heterogeneity along with exposure to polar groups. In this regard, the contact angles of  $\sim 76^\circ$  indicate moderate wettability, clearly confirming increased hydrophilicity compared to SF alone [48, 49]. With the further addition of PEG (Figure 2d), the microstructure changes drastically, raising porosity and roughening the morphology. PEG is a very hydrophilic

polyether, and while it disturbs the SF secondary structure, it improves miscibility for the polymer blend. Being rich in hydroxyl groups, PEG chains build up surface hydrogen-bonding sites and directly lower the water contact angle to about  $36^\circ$ . PEG causes its associated rise in wettability by surface roughening, physical and chemical enhancement of hydrophilic functionality. PEG reduces crystallinity, thereby rendering the composite more penetrable to water molecules [50, 51]. The SF/LN/PEG/Cur sample (Figure 2e) features the most porous and highly heterogeneous morphology among all the composites examined. This results from the synergistic action of PEG and Cur; PEG enhances the surface hydrophilic nature of the composite material, whereas Cur provides further sites of the polarity supplied by phenolic hydroxyls and enolic ketones. Such polar groups participate in hydrogen bonding as well as  $\pi$ - $\pi$ -type interactions with both the SF protein backbone and cellulose-based LN; in effect, structural disruption on the microlevel occurs, which facilitates increased polarity at the surface. This sample reaches the lowest contact angle value amongst all samples, interpreting it as the most hydrophilic surface. Such a surface is under consideration for biomedical uses where activities such as moisture absorption, cell adhesion, and protein interaction are crucial, including wound healing and tissue scaffolding [52, 53]. Conversely, the SF/LN/Cur composite (Figure 2f) displays only minor alterations in surface morphology relative to SF/LN. Compared to PEG-containing composites, it is less porous and less heterogeneous at the surface. As Cur imparts hydrophilic functionality groups, this action comes into play only in the absence of the PEG effect of chain disruption, which might actually prevent such incorporation. The impaired contact angle of about  $78^\circ$  signifies a slight tendency to the wettable side, confirming that, by itself, Cur is unable to drastically alter either the structure or surface polarity of the blend for a marked improvement in hydrophilicity [53, 54, 55]. PEG, being amphiphilic with flexible chains of ether, can disrupt the SF/LN matrix to allow hydroxyl groups to protrude and have the surface more porous and water-accessible. Cur adds to the polar character of the surface through hydrogen bonding and aromatic interactions, but needs PEG to fully deliver its potential to enhance the contact angle.



**Fig. 2.** FESEM images of composite, a) SF, b) LN, c) SF/LN, d) SF/LN/PEG, e) SF/LN/PEG/Cur and f) SF/LN/Cur. Scale bars= 100  $\mu$ m

The hydrophilic or hydrophobic nature of biomaterials critically influences their biomedical performance, especially in wound healing. The blends prepared were assessed in terms of their surface wettability through static water contact angle measurements, as shown in Figure 3. It was shown that the pure SF films could have a contact angle around  $100^\circ$ , which indicated that these films were hydrophobic. This natural hydrophobicity, in fact, holds because of the presence of both  $\beta$ -sheet crystalline domains and micro-air pockets, which exist on the surface itself, in repelling water [56, 57]. This observation is consistent with heterogeneous wetting behaviour, where surface roughness enhances apparent

hydrophobicity. Hydrophobicity indeed will favour the clots from the region that are thus not overly prone to moisture. Still, on the other hand, it would hinder cells from attaching and integrating with wet, lashed environments [13]. In contrast, due to the abundant presence of hydroxyl (-OH) groups that are ready to engage in hydrogen bonding with water molecules, LN is very hydrophilic [49]. The contact angle on LN was much less than that on SF, confirming its potential as a wettability-modifying agent. The contact angle of the SF/LN blend corresponds to a value between those of the two components, signalling the formation of intermolecular hydrogen bonds. Such interactions lead not only to the

increased miscibility of the mixture but also to improved water affinity, as more hydrophilic functional groups come nearer to the surface. The smaller contact angle of the SF/LN blend compared to the entirely pure SF is a clear sign of this biopolymer coupling effect. Then, the addition of curcumin (SF/LN/Cur) led to a further 28% decrease in the contact angle [54]. Due to its low water solubility, curcumin has a highly oxygenated structure, which can take part in hydrogen bonding with water. Such interactions, in addition to the amphiphilic character of Cur, might reduce the surface tension and promote enhanced water spreading across the surface [58]. The most critical improvement in hydrophilicity involved the SF/LN/PEG and SF/LN/PEG/Cur samples. Having a well-established reputation in the world of hydrophilic polymers has led to a significant increase in the hydroxyl group content on the surface. Compared to pure SF, the density of hydroxyl groups rose by nearly 38%, therefore placing an impressive 70% reduction in the angle of contact. The observation is in favour of earlier research that states PEG's ability to diminish the crystallinity and improve the uptake of the water [45, 50]. Notably, the SF/LN/PEG/Cur composite had the lowest contact angle of all samples tested. This is credited to the synergistic action of the hydrophilic chains present on PEG and the surface activity exhibited by Cur. The dual modification strategy thus succeeds in converting the SF/LN surface from hydrophobic to hydrophilic, which is highly useful for applications that require a high degree of water interaction, such as those in wound dressings, scaffolds for tissue engineering, and drug delivery carriers.

Figure 5, in contrast, presents two crucial

experimental characterizations: water uptake capacity (Figure 5b) and NIH3T3 fibroblasts viability (Figure 5b) after 5 days from the initiation of incubation, to extend the bulk-material-level performance and biological-interaction-level domains established by surface-level hydrophilicity (Figures 2–4). These parameters are indispensable in evaluation studies about the clinical potential of biomaterials in wound-healing applications requiring efficient fluid management and cellular sustenance. Water uptake data in Figure 5a coincide with and affirm the reported progressive change toward hydrophilicity observed from the contact angle measurements (Figure 3), yet also implicate the pertinence of bulk matrix spatial reconfiguration induced by chemical additives. Pure SF exhibited very scant water uptake, as expected, given that its  $\beta$ -sheet-dominated secondary structure results in chains packed so densely that very little porosity is generated, with a nonpolar surface that limits interaction with water and even restricts capillary ingress of water within the material, according to Wenzel's wetting model and the findings reported earlier by Fang et al. [55] and Lee et al. [44]. Upon LN incorporation, the water uptake showed a dramatic increase, which corresponds well with the high affinity between water and lignin hydroxyl groups. The LN matrix generates hydrophilic domains and potential sites for hydrogen bonding in the composite network, as suggested by FTIR shifts in the O–H and C–O stretching regions (Figure 1).

In fact, the enhanced roughness and porosity observed in FESEM images (Figure 2b, 2c) of these membranes contribute to their validity in terms of enhanced fluid permeability.

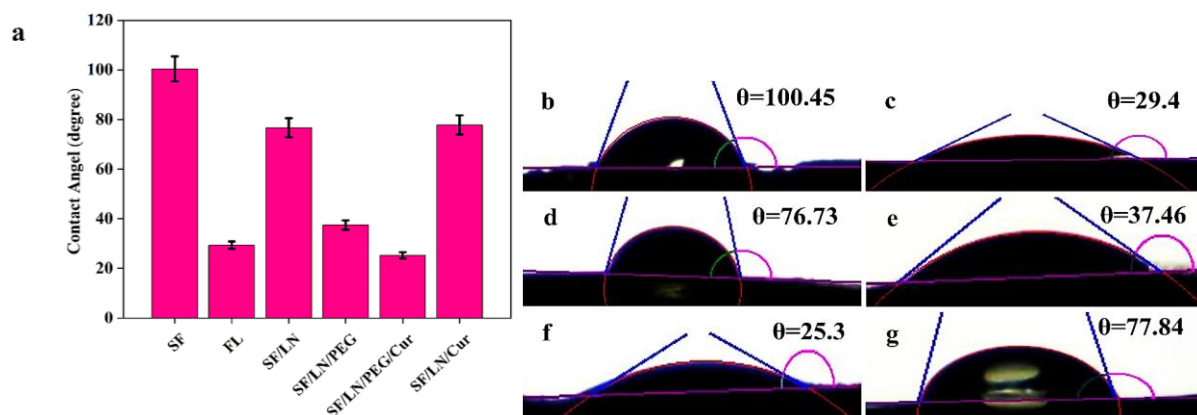


**Fig. 3.** The water wetting angles observed on various blend compositions: a) the average water wetting angle of SF/LN/PEG/Cur blends, b) SF, c) LN, d) SF/LN, e) SF/PEG, f) SF/LN/PEG/Cur and g) SF/LN/Cur

Increased water uptake occurs in the presence of PEG, in line with its chemical structure: repeating ether units (-CH<sub>2</sub>CH<sub>2</sub>O-), highly polar and flexible, enabling dynamic hydration shell formation around the polymer chains. PEG interferes with the crystallinity of SF (a decrease in the sharpness of amide peaks reveals this), increasing the volume fraction of amorphous regions and thus promoting water penetration. This is corroborated by the work of Gotoh et al. [50] and Pham et al. [51], who describe PEG as having the ability to create hydrophilic, porous morphologies in silk-based matrices. From the water absorption perspective, the SF/LN/PEG/Cur composite shows the maximum absorption rate. This synergistic enhancement occurs due to the loosening effect of PEG on the matrix and surface roughening that permits greater ingress and retention of aqueous media. The phenolic groups of curcumin provide extra polar interaction sites by hydrogen bonding and  $\pi$ - $\pi$  stacking, especially at the interfaces of SF and LN. While Cur, as in SF/LN/Cur, enhances water uptake only slightly over SF/LN, it remains unutilized mainly until the presence of PEG that further opens up the surface exposure of the functional groups and aids in the dispersion of Cur within the hydrophilic matrix.

This dual mode of additives reflects merely an additive-effect situation on the macroscale. At the same time, cooperativity at the molecular level allows the structural and chemical modifications to work against each other, ultimately improving hydrophilicity and fluid management potential. The relative viability of NIH3T3 fibroblast cells grown on varying composites of SF/LN after 5 days is plotted inside Figure 5b as a measure

of biocompatibility-labelling-head. For parallel purposes associated with any wound healing or tissue engineering scaffold. SF alone exhibits a truly low viable cell population despite being considered biocompatible [45]. This unintended behavior might be due to the impediment of adsorption of proteins needed to promote focal adhesion and cell spreading, brought about by factors such as the highly hydrophobic nature of  $\beta$ -sheet rich SF and its subsequently low surface energy [44, 56]. The absence of polarity at the SF matrix surface further restricts the adsorption of the key adhesion proteins, including fibronectin and vitronectin, that are vital in integrin attachment of cells to the substrate. Introduction of LN improves cell viability, the rationale unfolds being: enhanced surface polarity from hydroxyl groups, roughened morphology favorable to cellular anchoring (Figure 2b), and bioactivity of LN-based compounds (e.g., lignans and phenolics), which have been reported to exert anti-inflammatory and antioxidative benefits against adverse biological effects.

#### 4. CONCLUSIONS

This research established the fact that combining PEG and Cur with SF/LN mixtures increases their hydrophilicity, which is critical in applications for wound healing. Furthermore, FTIR studies demonstrated the formation of intermolecular hydrogen bonds among SF, LN, PEG, and Cur, verified through the shifts and intensity changes of characteristic absorption bands. The investigation through static water contact angle measurements displayed a clear trend:

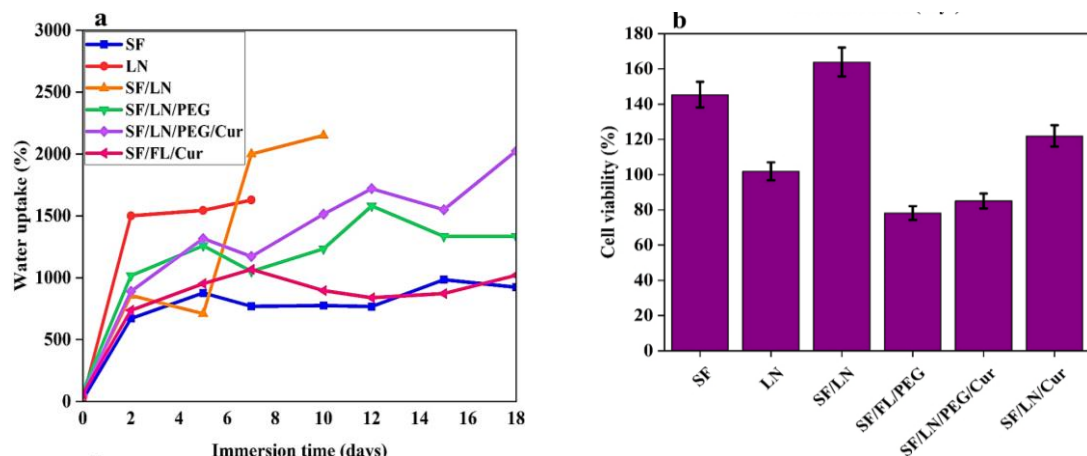


**Fig. 4.** a) water uptake percentage of different groups of composite SF/LN and b) The cell viability of NIH3T3 fibroblast cells cultured on composite after 5 day of cell culture

Pure silk fibroin had a hydrophobic surface with a contact angle close to 100°, while the inclusion of linen hydroxyl-rich structure lowered this value. Cur's addition further decreased the contact angle by ~28%, implying increased water affinity, while the most striking outcome was observed for PEG, which increased the concentration of hydroxyl groups approximately 380% compared with pure SF and decreased contact angle value by 70%. The SF/LN/PEG/Cur composite exhibited the lowest contact angle due to a highly hydrophilic surface that is, therefore, more amenable to water absorption and interaction with cells. The results in the study strongly support the synergism between PEG and Cur in changing SF/LN blends from hydrophobic to highly hydrophilic materials. Enhanced surface wettability, in turn, allows the flow of fluids through the dressing and supports cell proliferation while reducing dressing adhesion to wounds, thus paving the way for advanced wound care features. In the future, studies to be carried out include but aren't limited to studying the mechanical strength, degradation profile, and biocompatibility of these blends *in vitro* and *in vivo* to ensure clinical suitability for wound healing and tissue regeneration applications. It should be noted that the contribution of  $\pi$ - $\pi$  interactions remains speculative at this stage, as FTIR is not diagnostic for such interactions. Future work will employ spectroscopic techniques such as UV-Vis and fluorescence to explore this aspect in more detail.

## ACKNOWLEDGEMENTS

The authors are grateful for the support of Iran National Science Foundation (INSF) under the grant number 4024366.

## REFERENCES

- [1] Peña, OA. and Martin, P., "Cellular and molecular mechanisms of skin wound healing". *Nature Reviews Molecular Cell Biology.*, 2024, 25, 599-616.
- [2] Liao, Y., Zhang, Z., Zhao, Y., Zhang, S., Zha, K., Ouyang, L., et al. "Glucose oxidase: An emerging multidimensional treatment option for diabetic wound healing". *Bioactive Materials.*, 2025, 44, 131-51.
- [3] Sufiyan, M., Kushwaha, P., Ahmad, M., Mandal, P. and Vishwakarma, KK., "Scaffold-mediated drug delivery for enhanced wound healing: a review". *AAPS PharmSciTech.*, 2024, 25, 5-137.
- [4] Abdullah, H., "Sorrell CC: Preparation and characterisation of TiO<sub>2</sub> thick films by gel oxidation". In: *Materials Science Forum2007: Trans Tech Publ.*, 2007, 1, 2167-70.
- [5] Radulescu, D-M., Andronescu, E., Vasile, OR., Ficai, A. and Vasile, BS., "Silk fibroin-based scaffolds for wound healing applications with metal oxide nanoparticles". *Journal of Drug Delivery Science and Technology.*, 2024, 96, 105689.
- [6] Bogadi, S., Malayandi, R., Raj, PV., Kumar, PS., Parvathaneni, M., Kundu, MK., et al, "Silk fibroin and sericin: Multifunctional formulations for treating diabetic wound healing". *European Polymer Journal.*, 2024, 220, 113465.
- [7] Hassan, MA., Basha, AA., Eraky, M., Abbas, E. and El-Samad, LM., "Advancements in silk fibroin and silk sericin-based biomaterial applications for cancer therapy and wound dressing formulation: A comprehensive review". *International Journal of Pharmaceutics.*, 2024, 660, 124494.
- [8] Zhang, J., Wang, L., Xu, C., Cao, Y., Liu, S., Reis, RL. and et al., "Transparent silk fibroin film-facilitated infected-wound healing through antibacterial, improved fibroblast adhesion and immune modulation". *Journal of Materials Chemistry B.*, 2024, 12 2, 475-88.
- [9] Kaewpirom, S., Piboonnithikasem, S., Sroisroemsap, P., Uttoom and S., Boonsang, S., "Tailoring silk fibroin hydrophilicity and physicochemical properties using sugar alcohols for medical device coatings". *Scientific Reports.*, 2024, 14 1, 13781.
- [10] Yu, R., Yang, Y., He, J., Li, M. and Guo, B., "Novel supramolecular self-healing silk fibroin-based hydrogel via host-guest interaction as wound dressing to enhance wound healing". *Chemical Engineering Journal.*, 2021, 417, 128278.
- [11] Pagano, C., Baiocchi, C., Beccari, T., Blasi, F., Cossignani, L., Ceccarini, MR. and et al. "Emulgel loaded with flaxseed extracts as new therapeutic approach in wound treatment". 2021, 13 8, 1107.
- [12] Gębarowski, T., Jęskowiak, I. and Wiatrak,

B., "Investigation of the properties of linen fibers and dressings". *International Journal of Molecular Sciences.*, 2022, 23 18, 10480.

[13] Skórkowska-Telichowska, K., Mierziak-Darecka, J., Wrobel-Kwiatkowska, M., Gebrowski, T., Szopa, J. and Zuk, M., "Wound coverage by the linen dressing accelerates ulcer healing". *Advances in Dermatology and Allergology/Postępy Dermatologii i Alergologii.*, 2021, 38 5, 827-41.

[14] Ivanovska, A., Milenković, J., Lađarević, J., Mihajlović, K., Dojčinović, B., Ugrinović, V. and et al. "Harnessing the power of green and rooibos tea aqueous extracts for obtaining colored bioactive cotton and cotton/flax fabrics intended for disposable and reusable medical textiles". *Cellulose.*, 2024, 31 15, 9523-42.

[15] Kwiatkowska, E., Zimniewska, M., Gryszczyńska, A., Przybylska, P. and Różańska, W., "The Effect of Drought on the Content of Active Substances of Flax Fibers". *Journal of Natural Fibers.*, 2024, 21 1, 2310679.

[16] Deng, Y., Chen, J., Huang, J., Yang, X., Zhang, X., Yuan, S. and et al. "Preparation and characterization of cellulose/flaxseed gum composite hydrogel and its hemostatic and wound healing functions evaluation." *Cellulose.*, 2020, 27 7, 3971-88.

[17] Indrakumar, S., Dash, TK., Mishra, V., Tandon, B. and Chatterjee, K., "Silk Fibroin and Its Nanocomposites for Wound Care: A Comprehensive Review". *ACS Polymers Au.*, 2024, 4 3, 168-88.

[18] Baby, F., Vipin, K., Ibrahim, R., Asima, K. and Augusthy, AR., "SILK FIBROIN-APPLICATIONS IN MEDICAL TEXTILE". *Pharmaceutical Research.*, 2023, 13, 01.

[19] Shi, S., Wang, L., Song, C., Yao, L. and Xiao J., "Recent progresses of collagen dressings for chronic skin wound healing". *Collagen and Leather.*, 2023, 5 1, 31.

[20] Ahmad Shariff, SH., Daik, R., Haris, MS. and Ismail, MW., "Hydrophobic drug carrier from polycaprolactone-b-poly (Ethylene Glycol) star-shaped polymers hydrogel blend as potential for wound healing application". *Polymers.*, 2023, 15 9, 2072.

[21] Wang, Z., Zhao, Z., Khan, NR., Hua, Z., Huo, J. and Li, Y., "Microwave assisted chitosan-polyethylene glycol hydrogel membrane synthesis of curcumin for open incision wound healing". *Die Pharmazie-An International Journal of Pharmaceutical Sciences.*, 2020, 75 4, 118-23.

[22] Ao, F., Luo, X., Shen, W., Ge, X., Li, P., Zheng, Y. and et al. "Multifunctional electrospun membranes with hydrophilic and hydrophobic gradients property for wound dressing". *Colloids and Surfaces B: Biointerfaces.*, 2023, 225, 113276.

[23] Liao, HT., Lai, Y-T., Kuo, C-Y. and Chen J-P., "A bioactive multi-functional heparin-grafted aligned poly(lactide-co-glycolide)/curcumin nanofiber membrane to accelerate diabetic wound healing". *Materials Science and Engineering: C.*, 2021, 120, 111689.

[24] Adel, IM., ElMeligy, MF., Abdelkhalek, AA. and Elkasaby, NA., "Design and characterization of highly porous curcumin loaded freeze-dried wafers for wound healing". *European Journal of Pharmaceutical Sciences.*, 2021, 164, 105888.

[25] Soleimani, F., Pellerin, C., Omidfar, K. and Bagheri, R., "Engineered Robust Hydrophobic/Hydrophilic Nanofibrous Scaffolds with Drug-Eluting, Antioxidant, and Antimicrobial Capacity". *ACS Applied Bio Materials.*, 2024, 7 6, 3687-700.

[26] Behjati Hosseini, S., Arghavani, P., Hong, J., Rahimi, HR., Azad-Armaki, S., Yousefi, R. and et al., "Curcumin-loaded pickering emulsions based on soy protein isolate aggregates enhance diabetic wound healing". *Journal of Drug Delivery Science and Technology.*, 2024, 101, 106279.

[27] Johari, N., Madaah Hosseini, HR. and Samadikuchaksaraei, AJIPJ., "Mechanical modeling of silk fibroin/TiO<sub>2</sub> and silk fibroin/fluoridated TiO<sub>2</sub> nanocomposite scaffolds for bone tissue engineering". *Iranian Polymer Journal.*, 2020, 29 3, 219-24.

[28] Westhauser, F., Wilkesmann, S., Nawaz, Q., Hohenbild, F., Rehder, F., Saur, M. and et al., "Effect of manganese, zinc, and copper on the biological and osteogenic properties of mesoporous bioactive glass nanoparticles". *Journal of Biomedical Materials Research.*, 2021, 109 8, 1457-67.

[29] Alven, S., Nqoro, X. and Aderibigbe, BAJP., "Polymer-based materials loaded with

curcumin for wound healing applications". Advanced Polymeric Materials for Pharmaceutical Applications., 2020, 12 10, 2286.

[30] Deng, Y., Chen, J., Huang, J., Yang, X., Zhang, X., Yuan, S. and et al., "Preparation and characterization of cellulose/flaxseed gum composite hydrogel and its hemostatic and wound healing functions evaluation". *Cellulose.*, 2020, 27, 3971-88.

[31] Liu, J., Huang, R., Li, G., Kaplan, DL., Zheng, Z. and Wang, XJB., "Generation of nano-pores in silk fibroin films using silk nanoparticles for full-thickness wound healing". 2021; 22 2:546-56.

[32] Mohamadi, PS., Hivechi, A., Bahrami, SH., Nezari, S., Milan, PB. and Amoupour, MJBA., "Fabrication and investigating in vivo wound healing property of coconut oil loaded nanofiber/hydrogel hybrid scaffold". *Biomaterials Advances.*, 2022, 142, 213139.

[33] Hayes, JC. and Kennedy JEJMS, C E., "An evaluation of the biocompatibility properties of a salt-modified polyvinyl alcohol hydrogel for a knee meniscus application". *Materials Science and Engineering: C.*, 2016, 59, 894-900.

[34] Singh, V., Srivastava, D., Pandey, P., Kumar, M., Yadav, S., Kumar, DJJoDD. and et al., "Characterization, antibacterial and anticancer study of silk fibroin hydrogel". *Journal of Drug Delivery and Therapeutics.*, 2023, 13 2.

[35] Singh, V., Tripathi, DK., Sharma, VK., Srivastava, D., Kumar, U., Poluri, KM. and et al., "Silk fibroin hydrogel: A novel biopolymer for sustained release of vancomycin drug for diabetic wound healing". *Journal of Molecular Structure.*, 2023, 1286, 135548.

[36] Samant, L., Goel, A., Mathew, J., Jose, S. and Thomas, SJJoAPS., "Effect of surface treatment on flax fiber reinforced natural rubber green composite". *Journal of Applied Polymer Science.*, 2023, 140 12, e53651.

[37] Sathish, S., Kumaresan, K., Prabhu, L. and Gokulkumar, SJRRDM., "Experimental investigation of mechanical and FTIR analysis of flax fiber/epoxy composites incorporating SiC, Al<sub>2</sub>O<sub>3</sub> and graphite". *Romanian Journal of Materials.*, 2018, 48 4, 476.

[38] Zhang, W., Chen, L., Chen, J., Wang, L., Gui, X., Ran, J. and et al., "Silk fibroin biomaterial shows safe and effective wound healing in animal models and a randomized controlled clinical trial". *Advanced Healthcare Materials.*, 2017, 6 10, 1700121.

[39] Falqi, FH., Bin-Dahman, OA., Hussain, M. and Al-Harthi, MAJIIJoPS., "Preparation of miscible PVA/PEG blends and effect of graphene concentration on thermal, crystallization, morphological, and mechanical properties of PVA/PEG (10 wt%) blend". *The International Journal of Polymer Science.*, 2018, 1, 8527693.

[40] Nain, AKJTJoCT., "Unveiling the intermolecular interactions in ethyl acetate+ polyethylene glycol 200/300/400/600 binary mixtures by using densities, speeds of sound, excess properties and FTIR spectra at different temperatures". *The Journal of Chemical Thermodynamics.*, 2025, 201, 107391.

[41] Pham, DT., Le, TTD., Nguyen, NY., Duc, CKT., Tuan, NT., Luong, HVT. and et al. "PEGylated Silk Fibroin Nanoparticles for Oral Antibiotic Delivery: Insights into Drug–Carrier Interactions and Process Greenness". *ACS Omega.*, 2025, 10, 11, 11627–11641.

[42] Lai, D., Zhou, A., Tan, BK., Tang, Y., Hamzah, SS., Zhang, Z. and et al., "Preparation and photodynamic bactericidal effects of curcumin- $\beta$ -cyclodextrin complex". *Food Chemistry.*, 2021, 361, 130117.

[43] Ji, Z., Wei, T., Zhu, J., Hu, J., Xiao, Z., Bai, B. and et al., "Actively contractile and antibacterial hydrogel for accelerated wound healing". *Nano Research.*, 2024, 17 8, 7394-403.

[44] Radulescu, D-M., Andronescu, E., Vasile, OR., Ficai, A. and Vasile, BSJJoDDS., Technology. "Silk fibroin-based scaffolds for wound healing applications with metal oxide nanoparticles". *Journal of Drug Delivery Science and Technology.*, 2024, 1, 105689.

[45] Lee, JH., Park, BK. and Um, ICJIJoMS., "Preparation of highly crystalline silk nanofibrils and their use in the improvement of the mechanical properties of silk films". *International Journal of Molecular Sciences.*,

2022, 23 19, 11344.

[46] Atmakuri, A., Palevicius, A., Janusas, G. and Eimontas, JJP., "Investigation of hemp and flax fiber-reinforced EcoPoxy matrix biocomposites: morphological, mechanical, and hydrophilic properties". *Advanced Polymer-Based Sensors Materials.*, 2022, 14 21, 4530.

[47] Xia, X., Liu, W., Zhou, L., Hua, Z., Liu, H. and He, SJJP., "Modification of flax fiber surface and its compatibilization in polylactic acid/flax composites". *Iranian Polymer Journal.*, 2016, 25, 25-35.

[48] Kaewpirom, S., Piboonnithikasem, S., Sroisroemsap, P., Uttoom, S. and Boonsang, SJSR., "Tailoring silk fibroin hydrophilicity and physicochemical properties using sugar alcohols for medical device coatings". *Scientific Reports.*, 2024, 14 1, 13781.

[49] Lei, L., Zhao, B., Cheng, Z., Wei, Z., Ji, C., Zhu, Y. and et al., "Improving the interfacial adhesion and mechanical properties of flax fiber reinforced composite through fiber modification and layered structure". *Industrial Crops and Products.*, 2024, 221, 119305.

[50] Gotoh, Y., Tsukada, M., Minoura, N. and Imai, YJB., "Synthesis of poly (ethylene glycol)-silk fibroin conjugates and surface interaction between L-929 cells and the conjugates". *Biomaterials.*, 1997, 18 3, 267-71.

[51] Pham, DT., Le, TTD., Nguyen, NY., Duc, CKT., Tuan, NT., Luong, HVT. and et al., "PEGylated Silk Fibroin Nanoparticles for Oral Antibiotic Delivery: Insights into Drug–Carrier Interactions and Process Greenness". *ACS Omega.*, 2025, 10, 11627–11641.

[52] Mann, A., Lydon, F., Tighe, BJ., Suzuki, S. and Chirila TVJBp., "A study of the permeation and water-structuring behavioural properties of PEG modified hydrated silk fibroin membranes". *Biomedical Physics & Engineering Express.*, 2021, 7 4, 045002.

[53] Jaisamut, P., Wiwattanawongsa, K., Graidist, P., Sangsen, Y. and Wiwattanapatapee, RJAP., "Enhanced oral bioavailability of curcumin using a supersaturatable self-microemulsifying system incorporating a hydrophilic polymer; in vitro and in vivo investigations". *AAPS PharmSciTech.*, 2018, 19, 730-40.

[54] Heydari Foroushani, P., Rahmani, E., Alemzadeh, I., Vossoughi, M., Pourmadadi, M., Rahdar A, et al., "Curcumin sustained release with a hybrid chitosan-silk fibroin nanofiber containing silver nanoparticles as a novel highly efficient antibacterial wound dressing". *Nanomaterials.*, 2022, 12 19, 3426.

[55] Wang, H., Li, Z., Meng, Y., Lv, G., Wang, J., Zhang, D. and et al., "Co-delivery mechanism of curcumin/catechin complex by modified soy protein isolate: Emphasizing structure, functionality, and intermolecular interaction". *Food Hydrocolloids.*, 2024, 152, 109958.

[56] Fang, Y., Liu, Z., Jin, Y., Huang, Y., Zhou, S., Tian, H. and et al., "Electrospun high hydrophilicity antimicrobial poly (lactic acid)/silk fibroin nanofiber membrane for wound dressings". *International Journal of Biological Macromolecules.*, 2024, 277, 133905.

[57] Li, X., Qin, J. and Ma, JJRb., "Silk fibroin/poly (vinyl alcohol) blend scaffolds for controlled delivery of curcumin". *Regenerative Biomaterials.*, 2015, 2 2, 97-105.

[58] Iqbal, MA., Gohar, S., Zhu, C., Mayakrishnan, G. and Kim, ISJIJoBM., "Eggshell membrane as a novel and green platform for the preparation of highly efficient and reversible curcumin-based colorimetric sensor for the monitoring of chicken freshness". *International Journal of Biological Macromolecules.*, 2024, 266, 131089.